

Professor Alexander Laskin
Co-Editor of Atmospheric Chemistry and Physics

5 Dear Alex,

Listed below are our responses to the comments from the reviewers of our manuscript. We thank the reviewers for carefully reading our manuscript and for their very helpful suggestions! For clarity and visual distinction, the referee comments or questions are listed here in black and are preceded by bracketed, italicized numbers (e.g. *[1]*). Authors' responses are in red below each referee statement with matching numbers (e.g. *[A1]*).

Sincerely,

15 Allan Bertram
Professor of Chemistry
University of British Columbia

20 Anonymous Referee #1

The authors report about viscosity and diffusivity measurements of a brown carbon containing limonene SOA produced by ozonolysis under high mass loading conditions with subsequent exposure to ammonia. They report an increase in viscosity by 3-5 orders upon changing the water activity from 0.9 to dry and use the measured diffusion coefficient to deduce the mixing times for atmospheric particles. Their result suggest that mixing times are below 1 hour for PBL-conditions. This is in contrast to previous studies looking at SOA under low mass loading conditions which report significantly longer mixing times. The authors compare their viscosity data with their diffusivity data using the Stokes-Einstein relationship and conclude that it holds accurately for viscosities up to 10^4 Pa s.

This is a well-written manuscript and its topic is of core interest to the readers of ACP. It makes a very elegant use of the FRAP technique as it uses the BrC contained in the SOA as the fluorophore.

35 *[1]* However, the results suffer from being obtained under high mass loading conditions, which make them less relevant for direct applications to atmospheric SOA. As such the calculated mixing times likely provide a lower limit for atmospheric limonene SOA particles. I recommend to the authors to add a discussion whether it would be conceivable to use their technique also for brown LSOA produced at lower mass loading, so that the reader get a better feeling for the limits of the technique. I recommend publishing the paper as is.

[A1] The measurements reported in the original manuscript can be extended to lower mass loading conditions by using a multi-orifice impactor, which concentrates collected material into spots, and by collecting material for extended periods of time (e.g. several days) (Grayson et al., 2016). In response to the referee's comment, this information has been added to the end of the Summary and Conclusions of the revised manuscript.

Minor comments:

[2] - Abstract: While the authors acknowledge the problem of high mass loading here, I feel they should state explicitly that the magnitude of the difference in mixing times to more realistic SOA may be 3 orders of magnitude.

[A2] As suggested, in the abstract we have now explicitly stated that the mixing times may be 3 orders of magnitude longer.

[3] - Line 211: I am not entirely convinced by this argument. I agree that thermal steady state will be reached much quicker than the characteristic diffusion time. However, equally important may be the steady-state temperature difference. If significant, such a temperature difference may cause a redistribution of water molecules to outside of the irradiated region changing water activity locally. From the power density and thermal conductivity in the experiments the authors may estimate the temperature increase of the illuminated region.

[A3] Based on the laser power density and heat capacity of the sample and assuming no heat loss, the temperature increase for one image scan in the FRAP experiments will be ~ 1 K. In addition, the characteristic time for thermal diffusion when imaging is 30 ms. Since this characteristic time is much less than the imaging time, the temperature increase during scanning is expected to be less than ~ 1 K.

[4] - Line 253: I assume in Fig. 4, these are all above continents, correct?

[A4] Correct. More specifically, above the oceans, organic aerosol (OA) concentrations are almost always $\leq 0.5 \mu\text{g m}^{-3}$ according to predictions from GEOS-Chem (Figure 1 in Maclean et al. (Maclean et al., 2017)). Since we are only included conditions in Fig. 4 corresponding to when OA was $> 0.5 \mu\text{g m}^{-3}$ at the surface, Fig. 4 shows conditions almost exclusively for above continents. To address the referee's comment, we have add the following to Page 9:

“Based on this model, OA concentrations were almost always $< 0.5 \mu\text{g m}^{-3}$ above the surface of the oceans. Hence, Fig. 4 b-c do not include most conditions over the oceans.”

[5] - Caption of Fig. 5: Does the uncertainty for the calculated diffusivity include the uncertainty of the fluorophore radius?

85 [A5] Yes, except for the calculated diffusivity from Hinks et al. To address the referee's comments, we have modified Fig. 5 so that the uncertainty of the fluorophore radius is also included in the uncertainty for the calculated diffusivity from Hinks et al. We have also indicated in the caption of Fig. 5 that the calculated diffusivities include the uncertainty of the fluorophore radius.

Anonymous Referee #2

90 Summary:

'Viscosities, diffusion coefficients, and mixing times of intrinsic fluorescent organic molecules in brown limonene secondary organic aerosol and tests of the Stokes-Einstein equation' combines viscosity and diffusivity measurements across a range
95 of water activities for brown limonene SOA, and characterizes the accuracy of Stokes-Einstein relation for this system. The brown limonene SOA was generated using dark ozonolysis of d-limonene and then collected with an impactor and exposed to ammonia.

For the viscosity characterization, the authors used the bead-mobility technique for water activities higher than 0.7. For lower water activities, previously published data using
100 poke-flow techniques by Hinks et al. are used. For the diffusion coefficient and mixing time characterization, a nice aspect of the paper, the authors measure the diffusion coefficient of fluorescent molecules using 'rectangular area fluorescence recovery after photobleaching' (rFRAP). A thin film of brown LSOA was prepared between hydrophobic glass slides. A small area was then photobleached with a laser beam, and the fluorescence is allowed to recover by diffusion of fluorophores
105 into the photobleached region. The measurements in the study were used to test the accuracy of Stokes-Einstein relation, which is commonly used to infer diffusivity from viscosity measurements. It was found that the Stokes-Einstein relationship gave good agreement with measured values over several orders of magnitude in viscosity. This paper is well-written and the experiments well executed, with results useful for the community. There are some minor questions/comments listed below that the authors could better
110 address to improve the clarity of the paper.

Overall, I recommend publication in ACP.

Specific Comments"

115 [6] What is the chemical identity of the fluorophores (the "intrinsic fluorescent organic molecules") in brown limonene SOA? Are they present in other SOA? Can the diffusivity measurement used here be extended to other systems?

120 [A6] The exact molecular identities of the chromophores and fluorophores in brown LSOA is not known (see line 307-310 of the original version of the manuscript). It may be possible to extend these diffusion measurements to other systems that have intrinsic fluorescent organics, such as SOA produced from the photooxidation of aromatic compounds (Aiona et al., 2018). SOA from the photooxidation of aromatic

125 compounds contain fluorescent molecules, but experiments are needed to determine how readily these
130 molecules will photobleach in our experiments. Alternatively, to extend these measurements to other
SOA, we can add fluorescent dyes to the SOA matrix, and use these fluorescent dyes for the FRAP
measurements.

[7] Consider very briefly explaining the poke-flow technique for the uninitiated reader,
130 with description of limitations and uncertainties, since the results are used at low water
activities.

[A7] To address the referee's comment, a brief description of the poke-flow technique, as well as
135 limitations and uncertainties of the technique, has been added to the revised manuscript. Specifically, the
following text has been added to Section 2.2:

“Briefly, brown LSOA was collected on hydrophobic glass surfaces using a procedure similar to the
procedure described above. This resulted in supermicron particles with a spherical cap geometry. The
140 particles were then poked with a sharp needle, generating a half-torus geometry. After poking, the
material flowed and returned to its spherical cap geometry due to surface tension forces. From simulations
of fluid flow, the viscosities of the material were determined. This technique is limited to viscosities \geq
 10^3 Pa s. In addition, the upper and lower limits of viscosity differ by roughly a factor of 15 to 150. This
uncertainty stems mainly from uncertainties in the parameters used when simulating the fluid flow.”

[8] A schematic of the rFRAP technique/set-up, central to this paper, would be appreciated in the SI.
145 Additionally, the SI would be more instructive if it includes details of the thin-film preparation process,
with illustrative images of the slides after preparation. Also, can the authors comment on why 2D FRAP
was used, instead of the more traditional 1D FRAP? Is there some advantage? If 2D is somehow better,
why rectangular, and not circular (for symmetry, which would likely simplify the analysis).

[A8] A schematic of the rFRAP technique and slide after preparation has been included to the SI as
150 requested.

For 1D FRAP, I assume the referee is referring to measurements that include just temporal information.
155 In this case, knowledge of the initial bleaching profile is needed, which can be difficult to determine
accurately. For 2D FRAP, rectangular FRAP was chosen over circular FRAP since rectangular FRAP
has a closed-form expression for the recovery process. To clarify, in Section 2.3.2 of the revised
manuscript, we have mentioned the benefit of rectangular FRAP over circular FRAP.

[9] Line 178 - Why were the bleach and image sizes chosen based on water activity? Is there a calibration
160 curve for water activity versus area bleached? Does changing the
area affect the time of measurement?

[A9] The recovery time in rFRAP experiments is related to both the photobleaching area and diffusion
165 rate. When the diffusion rate was fast (e.g. high water activities), we used a larger photobleaching area,

and when the diffusion rate was slow (e.g. low water activities), we used a smaller photobleaching area to give experimentally accessible recovery times. To address the referee's comment, we have added this information to section 2.3.2 of the revised manuscript. Specifically the following was added:

170 “The recovery time in the rFRAP experiments were related to both the photobleaching area and diffusion
rate. When the diffusion rate was fast (e.g. high water activities), we used a larger photobleaching area,
and when the diffusion rate was slow (e.g. low water activities), we used a smaller photobleaching area
to give experimentally accessible recovery times.”

175 [10] Line 28 of the abstract contains the abbreviation ‘PBL’ without first being defined (it
is defined later in the introduction. Additionally, the term ‘LSOM’ has been used in the
figures and SI, but LSOA is used in the main manuscript.

180 [A10] Thank you for catching these mistakes. They have been corrected in the revised manuscript.

References:

185 Aiona, P. K., Luek, J. L., Timko, S. A., Powers, L. C., Gonsior, M., and Nizkorodov, S. A.: Effect of Photolysis on
Absorption and Fluorescence Spectra of Light-Absorbing Secondary Organic Aerosols, *Acs Earth and Space
Chemistry*, 2, 235-245, 10.1021/acsearthspacechem.7b00153, 2018.
Grayson, J. W., Zhang, Y., Mutzel, A., Renbaum-Wolff, L., Boege, O., Kamal, S., Herrmann, H., Martin, S. T., and
190 Bertram, A. K.: Effect of varying experimental conditions on the viscosity of alpha-pinene derived secondary
organic material, *Atmospheric Chemistry and Physics*, 16, 6027-6040, 10.5194/acp-16-6027-2016, 2016.
Maclean, A. M., Butenhoff, C. L., Grayson, J. W., Barsanti, K., Jimenez, J. L., and Bertram, A. K.: Mixing times of
organic molecules within secondary organic aerosol particles: a global planetary boundary layer perspective,
Atmospheric Chemistry and Physics, 17, 13037-13048, 10.5194/acp-17-13037-2017, 2017.

195

Viscosities, diffusion coefficients, and mixing times of intrinsic fluorescent organic molecules in brown limonene secondary organic aerosol and tests of the Stokes- Einstein equation

200 Dagny A. Ullmann¹, Mallory L. Hinks², Adrian Maclean¹, Christopher Butenhoff³, James Grayson¹,
Kelley Barsanti⁵, Jose L. Jimenez⁴, Sergey A. Nizkorodov², Saeid Kamal¹, Allan K. Bertram¹

¹Department of Chemistry, University of British Columbia, Vancouver, BC, V6T 1Z1, Canada

²Department of Chemistry, University of California, Irvine, CA 92697, USA

³Department of Physics, Portland State University, Portland, Oregon, USA

205 ⁴Cooperative Institute for Research in the Environmental Sciences and Department of Chemistry and Biochemistry, University
of Colorado, Boulder, CO, USA

⁵Department of Chemical and Environmental Engineering and Center for Environmental Research and Technology, University of California, Riverside, CA, USA

210 Correspondence to: Allan K. Bertram (bertram@chem.ubc.ca) and Saeid Kamal (skamal@chem.ubc.ca)

Abstract.

215 Viscosities and diffusion rates of organics within secondary organic aerosol (SOA) remain uncertain. Using the bead-mobility technique, we measured the viscosities as a function of water activity (a_w) of SOA generated by the ozonolysis of limonene followed by browning by exposure to NH_3 (referred to as brown limonene SOA or brown LSOA). These measurements together with viscosity measurements reported in the literature show that the viscosity of brown LSOA increases by 3-5 orders of magnitude as the a_w decreases from 0.9 to approximately 0.05. In addition, we measured diffusion coefficients of intrinsic fluorescent organic molecules within brown LSOA matrices using rectangular area fluorescence recovery after photobleaching.

220 Based on the diffusion measurements, as the a_w decreases from 0.9 to 0.33, the average diffusion coefficient of the intrinsic fluorescent organic molecules decreases from $5.5 \cdot 10^{-9} \text{ cm}^2 \text{ s}^{-1}$ to $7.1 \cdot 10^{-13} \text{ cm}^2 \text{ s}^{-1}$ and the mixing times of intrinsic fluorescent organic molecules within 200 nm brown LSOA particles increases from 0.002 s to 14 s. These results suggest that the mixing times of large organics in the brown LSOA studied here are short (< 1 hr) for a_w and temperatures often found in the ~~planetary boundary layer~~. Since the diffusion coefficients and mixing times reported here correspond to SOA generated using a high mass loading ($\sim 1,000 \mu\text{g m}^{-3}$), biogenic SOA particles found in the atmosphere with mass loadings $\leq 10 \mu\text{g m}^{-3}$ are likely to have higher viscosities and longer mixing times (possibly 3 orders of magnitude longer). These new measurements of viscosity and diffusion were used to test the accuracy of the Stokes-Einstein relation for predicting diffusion rates of organics within brown LSOA matrices. The results show that the Stokes-Einstein equation gives accurate predictions of diffusion coefficients of large organics within brown LSOA matrices when the viscosity of the matrix is as high as 10^2 to 10^4 Pa s. These results

225

230 have important implications for predicting diffusion and mixing with SOA particles in the atmosphere.

Deleted: PBL

1 Introduction

235 Large amounts of volatile organic compounds, such as isoprene, limonene, and α -pinene from biogenic sources and aliphatic and aromatic compounds from anthropogenic sources are released into the atmosphere. These compounds can be oxidized by a complex series of atmospheric reactions to form lower-volatility products that condense to form secondary organic aerosols (SOA) (Hallquist et al., 2009; Kanakidou et al., 2005). SOA makes up approximately 30-70% of the mass of atmospheric particles (Kanakidou et al., 2005; Jimenez et al., 2009). Due to the hygroscopic nature of SOA, an important component of

240 SOA particles is water (Bateman et al., 2015; Hildebrandt Ruiz et al., 2015; Massoli et al., 2010). The amount of water in SOA

particles is determined by the relative humidity (RH); as the RH increases, the water activity (a_w) (and hence water content) in SOA particles increases to maintain equilibrium with the gas phase. SOA particles can influence climate either directly by absorbing or scattering sunlight or indirectly by acting as cloud condensation nuclei (CCN) or ice nuclei (IN) (Kanakidou et al., 2005; Murray et al., 2010; Solomon, 2007; Wang et al., 2012). SOA particles can also influence air quality and public health (Baltensperger et al., 2008; Jang et al., 2006; Poschl and Shiraiwa, 2015; Shiraiwa et al., 2017b).

Despite the importance of SOA particles in climate and air quality, their physicochemical properties remain poorly understood (Hallquist et al., 2009). This leads to uncertainties when predicting the role of SOA particles in atmospheric chemistry, climate, and air quality (Hallquist et al., 2009; Shiraiwa and Seinfeld, 2012; Shrivastava et al., 2017a; Zaveri et al., 2014). One physicochemical property that remains poorly known is the rate of diffusion of organics within SOA particles (Liu et al., 2016; Shiraiwa et al., 2013; Shrivastava et al., 2017a; Ye et al., 2016). Information on diffusion rates is needed to predict the reactivity and photochemistry of SOA particles (Chu and Chan, 2017; Davies and Wilson, 2015; Gržinić et al., 2015; Houle et al., 2015; Li et al., 2015; Lignell et al., 2014; Shiraiwa et al., 2011; Wang et al., 2015). Diffusion rates are also needed to predict the growth rates, size distributions, cloud condensation ability, and ice nucleating ability of SOA particles (Boyd et al., 2017; Huff Hartz et al., 2005; Murray et al., 2010; Perraud et al., 2012; Riipinen et al., 2011; Shiraiwa and Seinfeld, 2012; Solomon and (eds.), 2007; Taina et al., 2017; Wagner et al., 2017; Wang et al., 2012; Zaveri et al., 2014; Zaveri et al., 2018). Slow diffusion of molecules in particles also has implications for the long-range transport of pollutants (Bastelberger et al., 2017; Shrivastava et al., 2017b; Zelenyuk et al., 2012; Zhou et al., 2012) and the optical properties of particles (Adler et al., 2013; Robinson et al., 2014).

To estimate diffusion rates of organics in SOA particles, it is common to use viscosity measurements together with the Stokes-Einstein relation (Booth et al., 2014; Hosny et al., 2013; Koop et al., 2000; Power et al., 2013; Renbaum-Wolff et al., 2013a; Shiraiwa et al., 2011; Shiraiwa et al., 2017a; Song et al., 2015; Song et al., 2016),

$$D = \frac{kT}{6\pi\eta R_H} \quad (1)$$

where D is the diffusion coefficient of the diffusing species, k is the Boltzmann constant, T is the temperature, η is the dynamic viscosity and R_H is the hydrodynamic radius of the diffusing species. Until now, the accuracy of the Stokes-Einstein relation for predicting diffusion rates of organics in SOA particles has not been quantified, leading to uncertainties when estimating diffusion rates from viscosity measurements. Motivated primarily by the food industry, there have been a few tests of the Stokes-Einstein relation for predicting diffusion rates of organics in organic-water matrices, such as saccharide-water matrices (Bastelberger et al., 2017; Champion et al., 1997; Chenyakin et al., 2017; Corti et al., 2008; Price et al., 2016). In these cases, the matrices contained only two species (one organic and water), which is very different from SOA matrices that contain thousands of different species (Nozière et al., 2015).

275 In the future, researchers will likely continue to use viscosity data combined with the Stokes-Einstein relation to estimate
diffusion rates of organics in SOA particles, because several techniques have been developed recently to measure the
viscosities of SOA matrices and proxies of SOA matrices (Bateman et al., 2015; Grayson et al., 2016b; Lee et al., 2017; Marsh
et al., 2017; Price et al., 2015; Reid et al., 2018; Renbaum-Wolff et al., 2013a; Song et al., 2015; Zhang et al., 2015). As a result,
the accuracy of the Stokes-Einstein relation for predicting diffusion rates of organics in SOA particles needs to be quantified.

280

In the following, we measured the viscosities of brown limonene SOA (brown LSOA) as a function of a_w using the bead-
mobility technique. The brown LSOA is a product of exposure of white limonene ozonolysis SOA to ppb levels of ammonia
vapour (Laskin et al., 2010), and it is a model system for the formation of secondary brown carbon (Laskin et al., 2015). In
addition, we measured diffusion coefficients of intrinsic fluorescent organic molecules within brown LSOA matrices using a
285 technique called rectangular area fluorescence recovery after photobleaching. These new data, combined with viscosity data
that already exist in the literature for brown LSOA-water matrices, were used to test the accuracy of the Stokes-Einstein relation
for predicting diffusion rates of organics within SOA particles. We also used the measured diffusion coefficients to estimate
mixing times of organics within 200 nm brown LSOA particles at RHs typically found in the planetary boundary layer (the
region of the atmosphere from the surface to an altitude of up to 1 km). We focused on brown LSOA for the following reasons:
290 first, brown LSOA contains light absorbing molecules that are also fluorescent (here referred to as intrinsic fluorescent organic
molecules) and capable of rapid photobleaching (Lee et al., 2013). These intrinsic fluorescent organic molecules offer a key
advantage because one can measure diffusion coefficients within brown LSOA using rectangular area fluorescence recovery
after photobleaching without the need to add a foreign tracer fluorescent molecule to the SOA matrix. Second, limonene
accounts for roughly 10 % of the global emissions of monoterpenes (and is thus an important source of SOA in the atmosphere)
295 (Kanakidou et al., 2005; Sindelarova et al., 2014).

2 Experimental

2.1 Generation of brown LSOA

Brown LSOA was produced at the University of California-Irvine (UCI) following the procedure outlined in Hinks
et al. (2016). First, particles consisting of limonene secondary organic material (LSOA) were generated in a 20 L flow tube by
300 dark ozonolysis of d-limonene. Mixing ratios of ozone and d-limonene (97% Sigma-Aldrich) were both 10 ppm prior to
reaction. Ozone was produced externally to the flow tube by an electric discharge in pure O₂ (Ultra High Purity, Airgas). After
the ozonolysis reaction, the mass concentration of LSOA particles within the flow tube was approximately 1,000 $\mu\text{g}/\text{m}^3$. At
the exit of the flow tube, the carrier gas and LSOA particles were passed through a charcoal denuder to eliminate excess ozone
and gas-phase organics, followed by collection of the LSOA particles on hydrophobic slides (Hampton Research; Aliso Viejo,
305 CA, USA) using a Sioutas impactor with a single stage “D” (0.25 μm cut point at 9 SLM collection flow rate). After LSOA
production, the hydrophobic slides containing the LSOA were placed within a small glass petri dish, which was left floating

on the surface of a solution of 0.1 M ammonium sulfate (>99 %, EMD) in a larger, covered petri dish. Over a period of three to five days, the ammonia vapour in equilibrium with the ammonium sulfate solution (concentration estimated to be 300 ppb NH₃ using the Extended AIM Aerosol Thermodynamics Model II) (Clegg et al., 1998) reacted with the fresh LSOA forming a visible brown colour. After production of the brown LSOA, the samples were shipped to the University of British Columbia for viscosity and diffusion coefficient measurements.

2.2 Viscosity measurements

The viscosities of brown LSOA particles were determined at a_w of approximately 0.7, 0.8 and 0.9, using the bead mobility technique (Renbaum-Wolff et al., 2013b). At lower a_w , the viscosities were too high for measurements with this technique. ~~In short, small particles (5-50 μm in diameter) of brown LSOA were deposited on fluorinated glass slides (Knopf, 2003) from the samples received from UCI using the tip of a needle (BD Precision Glide™ Needle, 0.9 mm x 40 mm). A dilute solution containing hydrophilic melamine beads (actual diameter: $(0.87 \pm 0.04) \mu\text{m}$, Sigma Aldrich, no. 86296) was then nebulized over the fluorinated glass slides containing the brown LSOA particles. This resulted in melamine beads being incorporated into the brown LSOA particles. The fluorinated glass slides containing the brown LSOA particles were then placed in a flow cell (Renbaum-Wolff et al., 2013b). The RH within the flow cell was controlled by passing a nitrogen carrier gas through a water bubbler, which was located in a temperature-controlled bath. The dew point of the nitrogen gas flow was measured with a hygrometer (General Eastern; Model 1311DR), and the temperature of the flow cell was measured with a thermocouple. From the dew point and the temperature of the flow cell, the RH was determined. The RH was calibrated at the beginning of each set of measurements using the deliquescence point of ammonium sulfate.~~

Once the fluorinated glass slides containing the brown LSOA particles were placed in the flow cell, a constant flow (1100 to 1200 sccm) of humidified nitrogen gas (Praxair, ultrapure) was passed over the brown LSOA particles, which caused a shear stress on the surface of the particles and circulation of the beads within the particles. The velocity of the beads was determined using an optical microscope (Zeiss Axio Observer). For each a_w studied, the speed of 7 to 16 beads in 2 to 5 brown LSOA droplets was measured and the bead speed was averaged. Once determined, the velocity of the beads was converted to viscosity using a calibration curve based on sucrose-water particles and glycerol-water particles from Grayson et al. (2017)(Grayson et al., 2017). Prior to measuring the velocity of the beads in an experiment, the brown LSOA particles were equilibrated with the RH within the flow cell for approximately 20 min, which should be long enough to ensure equilibration (Section S1).

~~Viscosity for the same brown LSOA at a_w of 0.05 and 0.3 are available from previous poke-flow measurements by Hinks et al. (2016). Briefly, in these studies brown LSOA was collected on hydrophobic glass surfaces using a procedure similar to the procedure described above. This resulted in supermicron particles with a spherical cap geometry. The particles were then poked with a sharp needle, generating a half-torus geometry. After poking, the material flowed and returned to its spherical~~

Moved down [1]: but viscosity for the same brown LSOA at a_w of 0.05 and 0.3 are available from previous poke-flow measurements by Hinks et al. (2016).

Deleted: , but viscosity for the same brown LSOA at a_w of 0.05 and 0.3 are available from previous poke-flow measurements by Hinks et al. (2016).

Deleted: S

Moved (insertion) [1]

Deleted: but v

cap geometry due to surface tension forces. From simulations of fluid flow, the viscosities of the material were determined. This technique is limited to viscosities $\geq 10^3$ Pa s (Grayson et al., 2015). In addition, the upper and lower limits of viscosity from this technique differ by roughly a factor of 15 to 150. This uncertainty stems mainly from uncertainties in the parameters used when simulating the fluid flow.

2.3 Diffusion coefficient measurements

2.3.1 Generation of thin films of brown LSOA with a known a_w for the diffusion coefficient measurements

Brown LSOA contains light absorbing molecules that are also fluorescent and easily photobleachable (Lee et al., 2013). Diffusion coefficients of these intrinsic fluorescent organic molecules were determined using rectangle area fluorescence recovery after photobleaching (discussed below). For this technique, thin films (20-90 μm thick) containing brown LSOA with a known a_w were needed. To produce thin films of brown LSOA with a known a_w , particles of brown LSOA with diameters of 50-200 μm were deposited on hydrophobic slides from the samples received from the UCI using the tip of a needle (BD Precision GlideTM Needle, 0.9 mm x 40 mm). The super-micrometer brown LSOA particles were then located within a flow cell or sealed glass jar with controlled RH to set the a_w within the brown LSOA (at equilibration, a_w within the brown LSOA equals RH/100). The times used to condition the brown LSOA particles to the controlled RH are given in Table S1, ranging from 17 min to 1.5 months, and discussed in Section S1. After equilibration, the brown LSOA particles were sandwiched between two hydrophobic glass slides to generate a thin film of brown LSOA with a thickness of 20-90 μm . Assembly of the films occurred within a glove bag that had a RH set to match the RH used for conditioning the brown LSOA particles in order to ensure the a_w within the LSOA did not change during assembly of the films. The thickness of the films was controlled by aluminium spacers inserted between the two hydrophobic glass slides prior to assembly. After assembly, the brown LSOA within the thin films were isolated from the surrounding atmosphere using a layer of vacuum grease around the perimeter of the films. For further details, see Chenyakin et al. (2017) and Fig. S1.

Deleted: .

2.3.2 Measurements of diffusion coefficients

Fluorescence recovery after photobleaching (FRAP) has often been used to determine diffusion rates of fluorescent molecules in biological samples such as in the cytoplasm and nuclei of cells (Axelrod et al., 1976; Deschout et al., 2010; Jacobson et al., 1976; Meyvis et al., 1999; Seksek et al., 1997). To determine diffusion coefficients of the intrinsic fluorophores in the brown LSOA, we used a version of FRAP, referred to as rectangular area fluorescence recovery after photobleaching (rFRAP) (Deschout et al., 2010). rFRAP was chosen over circular FRAP, since rFRAP has a closed-form expression for the recovery process. In rFRAP, a rectangular region of a thin film containing fluorescent molecules is photobleached with a high intensity laser beam of a confocal laser scanning microscope (Fig S2). After photobleaching, the fluorescence signal within the photobleached region recovers due to diffusion of fluorescent molecules from outside the photobleached region into the

380 photobleached region. The recovery of the fluorescence signal over time is monitored and used to determine the diffusion
coefficient of the fluorescent molecules.

The rFRAP measurements were conducted with a laser scanning confocal microscope (Zeiss Axio Observer LSM 5 10 MP)
with a low numerical aperture objective (Zeiss EC-Plan Neofluar 10x, 0.3 numerical aperture) to ensure near uniform
385 photobleaching in the z-direction. One-dimensional scanning with a pixel dwell of 2.56 μs and an image scan time of 1.57 s
was used. The images were acquired with 512x512 pixels with a pinhole set to 80 μm . The scanning laser power was varied
between 17.0 to 42.6 μW depending on the fluorescence of the sample. In order to achieve a bleach depth (decrease in
fluorescence intensity) of 30-50 %, as suggested by Deschout et al. (2010) for rFRAP experiments, the laser power for
photobleaching was varied between 93 and 297 μW , depending on the sample (Deschout et al., 2010).

390

A rectangular area was used for photobleaching with length (x) and width (y). The recovery time in the rFRAP experiments
were related to both the photobleaching area and diffusion rate. When the diffusion rate was fast (e.g. high water activities),
we used a larger photobleaching area, and when the diffusion rate was slow (e.g. low water activities), we used a smaller
photobleaching area to give experimentally accessible recovery times. The image sizes used in the rFRAP experiments were

395

chosen in relation to the bleach size with larger image sizes used for larger bleach sizes. For example, at $a_w \geq 0.8$, photobleached
areas of 20 μm by 20 μm and image sizes of 199.6 μm by 199.6 μm were used, while at $a_w = 0.33$, photobleached areas of 5
 μm by 5 μm and 3 μm by 3 μm and image sizes of 30 μm by 30 μm were used. All rFRAP experiments were carried out at a
temperature of 294.5 \pm 1.0 K. Shown in Figure 1 are examples of images of brown LSOA films with a_w of 0.33, 0.6 and 0.9
recorded during rFRAP experiments.

400 2.3.3 Extraction of diffusion coefficients

Based on Fick's second law of diffusion, Deschout et al. (2010) developed the following equation to describe the fluorescence
intensities in thin films after photobleaching a rectangular area with a confocal microscope (Deschout et al., 2010):

$$\frac{F(x,y,t)}{F_0(x,y)} = 1 - \frac{K_0}{4} \left[\operatorname{erf} \left(\frac{x+l_x}{\sqrt{w(D,t,r)}} \right) - \operatorname{erf} \left(\frac{x-l_x}{\sqrt{w(D,t,r)}} \right) \right] \times \left[\operatorname{erf} \left(\frac{y+l_y}{\sqrt{w(D,t,r)}} \right) - \operatorname{erf} \left(\frac{y-l_y}{\sqrt{w(D,t,r)}} \right) \right], \quad (2)$$

where $F(x, y, t)$ is the fluorescence intensity at coordinate (x,y) and time t after photobleaching, $F_0(x, y)$ is the fluorescence
405 intensity at coordinate (x,y) prior to photobleaching, K_0 is the effective bleach depth, which describes the decrease of the
fluorescence intensity within the photobleached area, l_x and l_y are the lengths of the photobleached area, r is the lateral
resolution of the microscope, and D is the diffusion coefficient of the fluorescent molecules. The parameter $w(D, t, r)$ is given
by the following equation:

$$w(D, t, r) = r^2 + 4Dt. \quad (3)$$

410

Deleted: .

Deleted: , with smaller areas for longer diffusion times

Deleted:

In a first step of the analysis for the extraction of diffusion coefficients, the images recorded after photobleaching were normalized to an image recorded prior to photobleaching using the open source program ImageJ (Schneider et al., 2012). The resolution of the images was changed from 512x512 pixels to 128x128 pixels by averaging to reduce the noise. Then, Eq. 2 was used to extract $w(D, t, r)$ from each image. In the fitting procedure used to extract $w(D, t, r)$, K_0 as well as a normalization factor were left as free parameters. Next, $w(D, t, r)$ was plotted as a function of t and a straight line was fit to the data. The diffusion coefficient, D , was calculated from the slope of the straight line using a linear fit with Eq. (3). Examples of plots of $w(D, t, r)$ vs t are shown in Figure 2.

Equation 2 assumes that the only mechanism for recovery in the photobleached region is diffusion of unbleached molecules. The spontaneous recovery of the fluorescence signal without diffusion, referred to as reversible photobleaching, has been observed in previous studies at short timescales (Sinnecker et al., 2005; Stout and Axelrod, 1995; Verkman, 2003). To determine if this process occurred during our diffusion measurements with brown LSOA, a separate set of experiments was carried out. Particles of brown LSOA (40 to 90 μm in diameter) were conditioned to an a_w of 0.6 and the entire particle was photobleached until the fluorescence intensity decreased by between 17 and 47%. The photobleaching was performed across the entire particle in order to rule out fluorescence intensity recovery due to diffusion of fluorescent molecules. Within the first five seconds after photobleaching a small amount of the fluorescent signal recovered (1-3 % of the photobleached signal), which we attribute to reversible photobleaching. To ensure this process did not impact our diffusion measurements, the data recorded during the first five seconds after photobleaching in the rFRAP experiments were not included when determining diffusion coefficients.

Possible heating of the sample during photobleaching by the laser was not expected to impact the diffusion measurements since local heating during photobleaching should be dissipated to the surroundings much faster than the time of the diffusion measurements. Nevertheless, to support this expectation, two experiments were carried out with different laser intensities but on the same sample conditioned to an a_w to 0.9. A laser intensity of 139.9 μW was used for a bleach depth of 20% and a laser intensity of 330 μW was used for a bleach depth of 50%. Within uncertainty, the diffusion coefficients determined with both bleach depths were in agreement: $(2.5 \pm 0.5) \cdot 10^{-9} \text{ cm}^2 \text{ s}^{-1}$ was obtained for a laser intensity of 139.9 μW and $(2.8 \pm 0.1) \cdot 10^{-9} \text{ cm}^2 \text{ s}^{-1}$ for a diffusion coefficient was obtained for a laser intensity of 330 μW (uncertainties correspond to 95 % confidence intervals).

Equation 2 assumes that the fluorescence intensity is proportional to the concentration of the intrinsic fluorescent molecules, which is a valid assumption when the transmittance of light through the samples is $\geq 95\%$ (Fonin et al., 2014). In our experiments the transmittance of light through the samples was $\leq 93\%$. To take into account the non-linearity between the fluorescence signal and concentration, the measured fluorescence signal was first converted to concentration using the following equation:

$$\frac{C(x,y,t)}{C_0(x,y)} = \frac{\log\left[1 - (1 - T_0) \frac{F(x,y,t)}{F_0(x,y)}\right]}{\log(T_0)}, \quad (4)$$

445 where $\frac{C(x,y,t)}{C_0(x,y)}$ is the normalized concentration of the intrinsic fluorescent dye, $\frac{F(x,y,t)}{F_0(x,y)}$ is the normalized fluorescence signal, and T_0 is the transmittance prior to the photobleaching process. Equation 4 is derived in Section S2. After the normalized concentrations were calculated, they were used in Eq. 2 in place of the normalized fluorescence signal. Note, the application of Eq. 4 to account for non-linearity between the fluorescence signal and concentration changed the diffusion coefficients by less than the uncertainties in the measurements.

450 **3 Results and Discussion**

3.1 Viscosity of brown limonene SOA

Figure 3 shows the viscosity of brown LSOA as a function of a_w measured with the bead-mobility technique. For comparison, the known viscosity of pure water and the viscosity of brown LSOA measured previously using the poke-and-flow technique are also included (Hinks et al., 2016). Overall, Figure 3 shows that the viscosity increases by 3-5 orders of magnitude as the a_w decreases from 0.9 to approximately 0.05. An increase in viscosity with a decrease in a_w is expected due to the plasticizing effect of water (Koop et al., 2011; Power et al., 2013; Zobrist et al., 2011). A liquid has a viscosity of $< 10^2$ Pa·s, a semisolid has a viscosity of 10^2 and 10^{12} Pa·s, and an amorphous solid has a viscosity of $> 10^{12}$ Pa·s (Koop et al., 2011; Mikhailov et al., 2009; Shiraiwa et al., 2011). Based on Figure 3, the brown LSOA studied here can be considered as a liquid above a a_w of 0.7, and as a semisolid at a_w below roughly 0.5.

460 **3.1 Diffusion coefficients and mixing times of intrinsic fluorophores in brown limonene SOA**

Figure 4(a) shows the measured diffusion coefficients of the intrinsic fluorophores in brown LSOA as a function of a_w . The average diffusion coefficient decreases from $5.5 \cdot 10^{-9}$ cm²/s to $7.1 \cdot 10^{-13}$ cm²/s as the a_w decreases from 0.9 to 0.33. The strong dependence on a_w is due to the plasticizing effect of water as mentioned above (Koop et al., 2011; Power et al., 2013; Zobrist et al., 2011). Also included in Figure 4 (secondary y-axis) is the mixing time of the intrinsic fluorophores by molecular diffusion within a 200 nm brown SOA particle based on the measured diffusion coefficients. Mixing times were calculated with the following equation (Seinfeld and Pandis, 2016; Shiraiwa et al., 2011):

$$\tau_{mixing} = \frac{D_p^2}{4\pi^2 D_{org}}, \quad (5)$$

where D_p is the diameter of the particle and D_{org} the measured diffusion coefficient of the intrinsic fluorophore. The mixing time is the time after which the concentration of the diffusing molecules at the centre of the particle deviates by less than 1/e from the equilibrium concentration (Shiraiwa et al., 2011). Based on the measured diffusion coefficients, for the brown LSOA studied here mixing times of the organics within 200 nm particles range from 0.002 s to 14 s for a_w from 0.9 to 0.33.

Also shown in Figure 4 is the frequency distributions of a_w (Panel b) and temperatures (Panel c) found in the planetary boundary layer (PBL) for the months of January and July. We calculated these frequency distributions using GEOS-Chem version v10-

475 01 (Pye et al., 2010), which was driven by 6-hr average GEOS-5 meteorology fields. Following Maclean et al. (2017), when
determining the frequency distributions of a_w and temperatures within the PBL, we only included grid cells in a column up to
the top of the PBL if the monthly averaged concentrations of organic aerosol (OA) were $> 0.5 \mu\text{g m}^{-3}$ at the surface, based on
GEOS-Chem version v10-01 (Pye et al., 2010). **Based on this model, OA concentrations were almost always $< 0.5 \mu\text{g m}^{-3}$
480 above the surface of the oceans. Hence, Fig. 4 b-c do not include most conditions over the oceans.** We excluded cases when
OA concentrations were $< 0.5 \mu\text{g m}^{-3}$ at the surface since these concentrations are not expected to be important for climate or
health. OA concentrations were $> 0.5 \mu\text{g m}^{-3}$ in all but one of the previous surface measurements of OA at remote locations
(Spracklen et al., 2011).

Figure 4(b) shows that a_w in the PBL is most often ≥ 0.33 when the organic mass concentrations are higher than $0.5 \mu\text{g m}^{-3}$ at
485 the surface. Figure 4(c) shows that the temperature in the PBL is often within 5 K of the temperature used in our experiments
(294.5 K). Based on Figure 4, mixing times of intrinsic fluorophore in the brown LSOA studied here are often short (< 1 h)
for a_w -values and temperatures most often found in the PBL when the organic mass concentrations are higher than $0.5 \mu\text{g m}^{-3}$.

The diffusion coefficients and mixing times reported here correspond to brown LSOA generated using mass concentrations
490 of $1,000 \mu\text{g m}^{-3}$ in a flow reactor. For some types of SOA (SOA from ozonolysis of α -pinene, limonene, 3-hexenyl acetate and
3-hexen-1-ol) the viscosity of the SOA increases as the mass concentration used to generate the SOA decreases (Grayson et
al., 2016; Jain et al., 2018). Since mass concentrations of biogenic SOA particles found in the atmosphere are most often
 $\leq 10 \mu\text{g m}^{-3}$ (Spracklen et al., 2011) the values reported here likely represent the lower limit for the viscosities and upper limit
495 for the diffusion coefficients. Additional studies are needed to determine diffusion coefficients and mixing times for more
atmospherically relevant mass concentrations. In addition, the brown LSOA were generated using a ratio of limonene to ozone
 ~ 1 , which suggests that not all double bonds in limonene were oxidized. Additional studies are also needed to determine if
diffusion coefficients in brown LSOA are sensitive to the extent of oxidation of LSOA molecules.

Ye et al. (2018) studied the timescale for mixing of organics from toluene oxidation within limonene SOA particles using mass
500 spectrometry (Ye et al., 2018). In these studies, the limonene SOA particles were generated with mass concentration of 16-22
 $\mu\text{g m}^{-3}$. Based on the studies by Ye et al. (2018) the mixing times of organics within limonene SOA particles is on the order
of 3-4 hr for RH values ranging from 10 to 30%, with little evidence for an RH dependence. At 33% RH, we calculate a
mixing time of approximately 14 s. This corresponds to a difference in diffusion coefficients of a factor of roughly 1000. A
possible explanation for the apparent difference between the current results and the results reported by Ye et al. (2018) is the
505 difference in the mass concentrations used to generate the SOA, and the low extent of oxidation of LSOA compounds, as
discussed above.

Formatted: Font: (Default) +Headings (Times New Roman),
10 pt

Formatted: Font: 10 pt

Formatted: Font: (Default) +Headings (Times New Roman),
10 pt

Field Code Changed

Formatted: Font: (Default) +Headings (Times New Roman),
10 pt

Formatted: Font: 10 pt

Formatted: Font: (Default) +Headings (Times New Roman)

Field Code Changed

Deleted: the

Deleted: the

510 3.4. Comparison between measured diffusion coefficients and Stokes-Einstein predictions

Shown in Figure 5 are the measured diffusion coefficients and predicted diffusion coefficients based on viscosity measurements and the Stokes-Einstein relation. The viscosity measurements include our new bead-mobility viscosity results (Figure 3) and previous poke-flow viscosity measurements by Hinks et al. (2016), as well as viscosity measurements of pure water for comparison (Crittenden et al., 2012;Hinks et al., 2016). To predict diffusion coefficients from the viscosity measurements and the Stokes-Einstein equation, the average dimension of the intrinsic fluorophores is needed. The exact molecular identities of the chromophores and fluorophores in brown LSOA is not known. Previous studies suggest that there is a distribution of chromophores with a broad range of molecular weights of the order of 500 g/mol (Nguyen et al., 2013). Therefore, we tested a range of molecular weights from 300 to 800 g/mol, corresponding to hydrodynamic radii from 4.5 to 6.2 Å with an assumed density of 1.3 g/cm³ (Saathoff et al., 2009), and an assumed spherical geometry of the intrinsic fluorophores.

Figure 5 shows that the difference between the measured and predicted diffusion coefficients is less than the uncertainty of the measurements for diffusion coefficients as small as roughly 10⁻¹² cm² s⁻¹, which corresponds to a viscosity of between 4·10² to 1.2·10⁴ Pa·s, based on Figure 4. This conclusion is consistent with most previous studies that have investigated the accuracy of the Stokes-Einstein relation for predicting diffusion coefficients of large organic molecules in organic-water mixtures. For example, Chenyakin et al. (2017), Champion et al. (1997), and Price et al. (2016) showed that the Stokes-Einstein relation predicts diffusion coefficients of large organics in sucrose-water solution consistent with measurements (i.e., within the uncertainty of the measurements) when the viscosity is $\lesssim 1\cdot 10^4$ Pa·s (Champion et al., 1997;Chenyakin et al., 2017;Price et al., 2016). In contrast, Longinotti and Corti (2007) and Corti et al. (2008) found disagreement between measured and predicted diffusion coefficients of large organics in organic-water solutions at slightly lower viscosities (Corti et al., 2008;Longinotti and Corti, 2007).

4 Summary and conclusion

One physicochemical property of SOA particles that remains poorly understood is diffusion rates of representative organics within SOA particles. To estimate diffusion rates of organics in realistic models for SOA particles, we (as well as other researchers) have used viscosity measurements together with the Stokes-Einstein relation. Until now, the accuracy of the Stokes-Einstein relation for predicting diffusion coefficients of organics in SOA particles had not been quantified, leading to uncertainties when estimating diffusion rates from viscosity measurements. In this study, we measured the viscosity of brown LSOA using the bead mobility technique. From these viscosity values, we calculated diffusion coefficients of large organic molecules in brown LSOA. These calculated diffusion coefficient values were compared to diffusion coefficients of large organic molecules that were measured directly in brown LSOA using fluorescence recovery after photobleaching. We found

that the Stokes-Einstein relation gives diffusion coefficients within the uncertainty of the measurements for brown LSOA matrices with viscosities between 0.2 Pa·s and 1.2·10⁴ Pa·s.

545 In addition, mixing times in a 200 nm sized brown LSOA particle were calculated based on the measured diffusion coefficients. Mixing times were found to vary between 0.001 s at an a_w of 0.9 and 14 s at an a_w of 0.3. These results suggest that the mixing times of large organics in the brown LSOA studied here are short (< 1 h) for a_w and temperatures often found in the PBL. However, since the mixing times reported here correspond to brown LSOA generated using mass loadings of 1,000 $\mu\text{g m}^{-3}$, the mixing times are likely to be longer in ambient biogenic SOA particles typically found at mass loadings below 10 $\mu\text{g m}^{-3}$
550 (Spracklen et al., 2011). Additional studies are needed using more atmospherically relevant mass concentrations, as well as utilizing a range of oxidation conditions from “fresh” to “highly-aged” SOA. The measurements reported here can be extended to lower mass loading conditions by using a multi-orifice impactor, which concentrates collected material into spots, and by collecting material for extended periods of time (e.g. several days) (Grayson et al., 2016a).

5 Acknowledgement

555 This work was funded by the Natural Science and Engineering Research Council of Canada. JIJ was supported by DOE (BER/ASR) DE-SC0016559. Support from the MJ Murdock Charitable Trust (grant 2012183) for computing infrastructure at Portland State University is acknowledged.

Formatted: Font: 10 pt, Not Italic

Formatted: Font: 10 pt, Not Italic, Font color: Auto

Formatted: Font color: Auto

Formatted: Font: 10 pt, Not Italic, Font color: Auto

Formatted: Font color: Auto

Formatted: Font: 10 pt, Not Italic, Font color: Auto

Formatted: Font color: Auto

Formatted: Font: 10 pt, Not Italic, Font color: Auto

Formatted: Font: 10 pt, Not Italic, Font color: Auto

Formatted: Font: 10 pt, Not Italic, Font color: Auto

Formatted: Font: Not Italic, Font color: Auto

560 7 Figures.

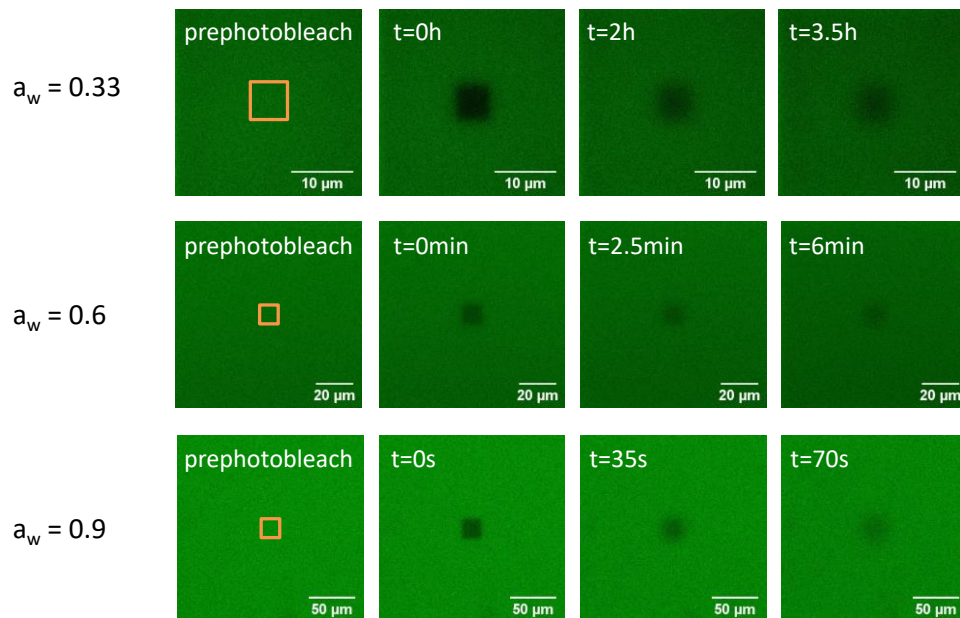
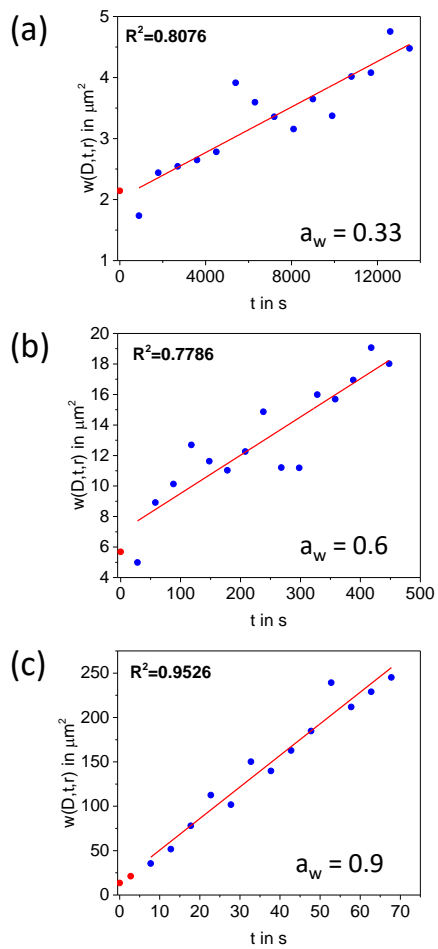


Figure 1: Images of brown limonene SOA films at three different a_w (0.33, 0.6 and 0.9) recorded during a rectangular fluorescence recovery after photobleaching (rFRAP) experiment. Times shown in each panel correspond to times after photobleaching. The orange rectangles depict the area to be photobleached.



565

Figure 2: Plot of $w(D,t,r)$ as a function of time at a_w of 0.9, 0.6 and 0.33. The red line is a linear fit to the data. The blue circles represent the data points that were included in the linear fit, the red circles represent data that were not included because of possible reversible photobleaching. The diffusion coefficients were obtained from the slopes.

570

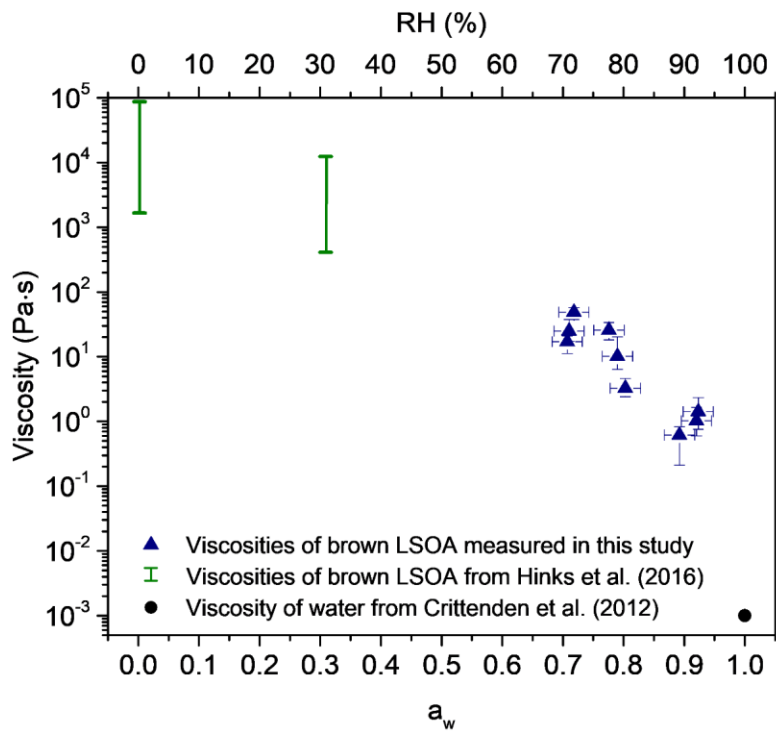
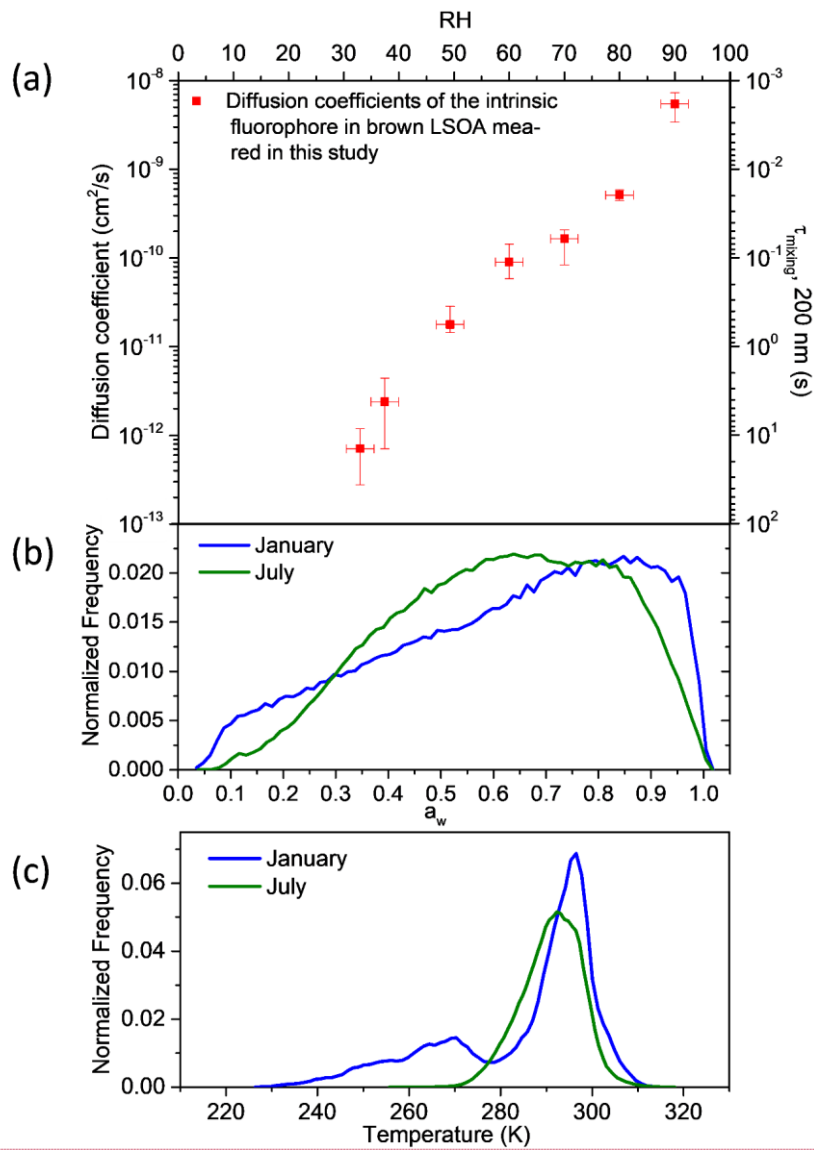


Figure 3: Viscosity of brown LSOA as a function of a_w (primary x-axis) and RH (secondary x-axis). The green bars show the viscosities that were measured by Hinks et al. (2016) and the blue triangles show the viscosities that were measured in this study using the bead mobility technique. The black circle is the viscosity of water measured by Crittenden et al. (2012).

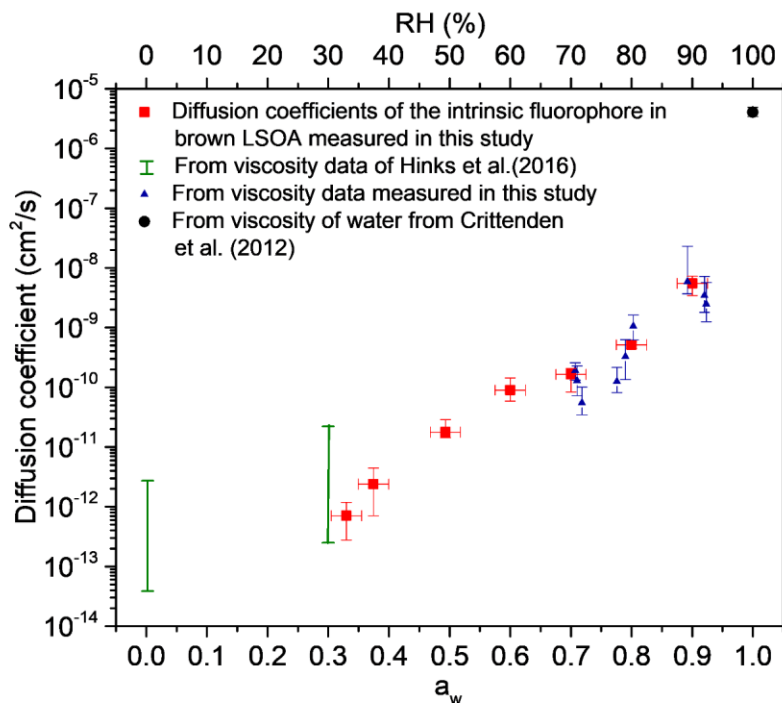
575



Deleted: ¶

585 **Figure 4: Panel (a):** measured diffusion coefficients of the intrinsic fluorophore in brown LSOA as a function of a_w (primary x-axis) and RH (secondary x-axis). The secondary y-axis shows the mixing time, which is the time that would be needed for intrinsic fluorophores to mix within a 200 nm brown limonene particle. The y-error bars correspond to the highest and lowest diffusion coefficient measured. The x-error bars correspond to uncertainty of the RH measurements ($\pm 2.5\%$). **Panel (b):** the a_w distribution in January (blue line) and July (green line) in the planetary boundary layer (PBL) when monthly averaged concentrations of organic aerosol (OA) are $>0.5 \mu\text{g m}^{-3}$ at the surface based on GEOS-Chem. **Panel (c)** the temperature distribution in January and July in the PBL when monthly averaged concentrations of OA are $>0.5 \mu\text{g m}^{-3}$ at the surface based on GEOS-Chem.

590
|



595

Figure 5: Measured and calculated diffusion coefficients in brown LSOA as a function of a_w (primary x-axis) and RH (secondary x-axis). The red squares show the measured diffusion coefficients of intrinsic fluorophores in brown LSOA. The blue triangles show the calculated diffusion coefficients of the intrinsic fluorophore in brown LSOA based on viscosities measured in this study using the bead mobility technique and the Stokes-Einstein equation. The y-error bars for the diffusion coefficients measured in this study (red squares) and the diffusion coefficients calculated from bead mobility viscosity measurements (blue triangles) show the highest and lowest values measured. The green vertical bars depict the highest and the lowest limit of calculated diffusion coefficients of brown LSOA based on viscosity measurements from Hinks et al. (2016) and the Stokes-Einstein equation. The black circle depicts the calculated diffusion coefficient of the intrinsic fluorophore in pure water based on viscosity measurements of Crittenden et al. (2012) and the Stokes-Einstein equation. The uncertainties for the calculated diffusion coefficients take into account the uncertainty of the hydrodynamic radii of the diffusing molecules (4.5 to 6.2 Å).

600

605

References

- Adler, G., Koop, T., Haspel, C., Taraniuk, I., Moise, T., Koren, I., Heiblum, R. H., and Rudich, Y.: Formation of highly porous aerosol particles by atmospheric freeze-drying in ice clouds, *Proceedings of the National Academy of Sciences*, 110, 20414-20419, 10.1073/pnas.1317209110, 2013.
- 615 Axelrod, D., Koppel, D. E., Schlessinger, J., Elson, E., and Webb, W. W.: Mobility measurement by analysis of fluorescence photobleaching recovery kinetics, *Biophysical Journal*, 16, 1055-1069, 10.1016/S0006-3495(76)85755-4, 1976.
- Baltensperger, U., Dommen, J., Alfarra, M. R., Duplissy, J., Gaeggeler, K., Metzger, A., Facchini, M. C., Decesari, S., Finessi, E., and Reimig, C.: Combined determination of the chemical composition and of health effects of secondary organic aerosols: the POLYSOA project, *Journal of aerosol medicine and pulmonary drug delivery*, 21, 145-154, 10.1089/jamp.2007.0655, 2008.
- 620 Bastelberger, S., Krieger, U. K., Luo, B., and Peter, T.: Diffusivity measurements of volatile organics in levitated viscous aerosol particles, *Atmos. Chem. Phys.*, 17, 8453-8471, 10.5194/acp-17-8453-2017, 2017.
- Bateman, A. P., Bertram, A. K., and Martin, S. T.: Hygroscopic Influence on the Semisolid-to-Liquid Transition of Secondary Organic Materials, *The Journal of Physical Chemistry A*, 119, 4386-4395, 10.1021/jp508521c, 2015.
- 625 Booth, A. M., Murphy, B., Riipinen, I., Percival, C. J., and Topping, D. O.: Connecting Bulk Viscosity Measurements to Kinetic Limitations on Attaining Equilibrium for a Model Aerosol Composition, *Environmental Science & Technology*, 48, 9298-9305, 10.1021/es501705c, 2014.
- Boyd, C. M., Nah, T., Xu, L., Berkemeier, T., and Ng, N. L.: Secondary Organic Aerosol (SOA) from Nitrate Radical Oxidation of Monoterpenes: Effects of Temperature, Dilution, and Humidity on Aerosol Formation, Mixing, and Evaporation, *Environmental Science & Technology*, 51, 7831-7841, 10.1021/acs.est.7b01460, 2017.
- 630 Champion, D., Hervet, H., Blond, G., Le Meste, M., and Simatos, D.: Translational Diffusion in Sucrose Solutions in the Vicinity of Their Glass Transition Temperature, *The Journal of Physical Chemistry B*, 101, 10674-10679, 10.1021/jp971899i, 1997.
- Chenyakin, Y., Ullmann, D. A., Evoy, E., Renbaum-Wolff, L., Kamal, S., and Bertram, A. K.: Diffusion coefficients of organic molecules in sucrose-water solutions and comparison with Stokes-Einstein predictions, *Atmos. Chem. Phys.*, 17, 2423-2435, 10.5194/acp-17-2423-2017, 2017.
- 635 Chu, Y., and Chan, C. K.: Reactive Uptake of Dimethylamine by Ammonium Sulfate and Ammonium Sulfate-Sucrose Mixed Particles, *The Journal of Physical Chemistry A*, 121, 206-215, 10.1021/acs.jpca.6b10692, 2017.
- Clegg, S. L., Brimblecombe, P., and Wexler, A. S.: Thermodynamic Model of the System $\text{H}^+ - \text{NH}_4^+ - \text{SO}_4^{2-} - \text{NO}_3^- - \text{H}_2\text{O}$ at 640 Tropospheric Temperatures, *The Journal of Physical Chemistry A*, 102, 2137-2154, 10.1021/jp973042r, 1998.
- Corti, H. R., Frank, G. A., and Marconi, M. C.: An Alternate Solution of Fluorescence Recovery Kinetics after Spot-Bleaching for Measuring Diffusion Coefficients. 2. Diffusion of Fluorescein in Aqueous Sucrose Solutions, *Journal of Solution Chemistry*, 37, 1593-1608, 10.1007/s10953-008-9329-4, 2008.
- 645 Crittenden, J. C., Trussell, R. R., Hand, D. W., Howe, K. J., and Tchobanoglous, G.: Physical and Chemical Quality of Water, in: *MWH's Water Treatment: Principles and Design*, Third Edition, John Wiley & Sons, Inc., 17-71, 2012.
- Davies, J. F., and Wilson, K. R.: Nanoscale interfacial gradients formed by the reactive uptake of OH radicals onto viscous aerosol surfaces, *Chemical Science*, 6, 7020-7027, 10.1039/c5sc02326b, 2015.
- Deschout, H., Hagman, J., Fransson, S., Jonasson, J., Rudemo, M., Lorén, N., and Braeckmans, K.: Straightforward FRAP for quantitative diffusion measurements with a laser scanning microscope, *Opt. Express*, 18, 22886-22905, 10.1364/oe.18.022886, 2010.
- 650 Fonin, A. V., Sulatskaya, A. I., Kuznetsova, I. M., and Turoverov, K. K.: Fluorescence of Dyes in Solutions with High Absorbance. Inner Filter Effect Correction, *PLoS ONE*, 9, e103878, 10.1371/journal.pone.0103878, 2014.

- Grayson, J. W., Song, M., Sellier, M., and Bertram, A. K.: Validation of the poke-flow technique combined with simulations of fluid flow for determining viscosities in samples with small volumes and high viscosities, *Atmos. Meas. Tech.*, 8, 2463-2472, 10.5194/amt-8-2463-2015, 2015.
- 655 Grayson, J. W., Zhang, Y., Mutzel, A., Renbaum-Wolff, L., Boege, O., Kamal, S., Herrmann, H., Martin, S. T., and Bertram, A. K.: Effect of varying experimental conditions on the viscosity of alpha-pinene derived secondary organic material, *Atmospheric Chemistry and Physics*, 16, 6027-6040, 10.5194/acp-16-6027-2016, 2016a.
- 660 Grayson, J. W., Zhang, Y., Mutzel, A., Renbaum-Wolff, L., Böge, O., Kamal, S., Herrmann, H., Martin, S. T., and Bertram, A. K.: Effect of varying experimental conditions on the viscosity of α -pinene derived secondary organic material, *Atmos. Chem. Phys.*, 16, 6027-6040, 10.5194/acp-16-6027-2016, 2016b.
- Grayson, J. W., Evoy, E., Song, M., Chu, Y., Maclean, A., Nguyen, A., Upshur, M. A., Ebrahimi, M., Chan, C. K., Geiger, F. M., Thomson, R. J., and Bertram, A. K.: The effect of hydroxyl functional groups and molar mass on the viscosity of non-crystalline organic and organic-water particles, *Atmos. Chem. Phys.*, 17, 8509-8524, 10.5194/acp-17-8509-2017, 2017.
- 665 Gržinić, G., Bartels-Rausch, T., Berkemeier, T., Türler, A., and Ammann, M.: Viscosity controls humidity dependence of N₂O₅ uptake to citric acid aerosol, *Atmos. Chem. Phys.*, 15, 13615-13625, 10.5194/acp-15-13615-2015, 2015.
- Hallquist, M., Wenger, J. C., Baltensperger, U., Rudich, Y., Simpson, D., Claeys, M., Dommen, J., Donahue, N. M., George, C., Goldstein, A. H., Hamilton, J. F., Herrmann, H., Hoffmann, T., Iinuma, Y., Jang, M., Jenkin, M. E., Jimenez, J. L., Kiendler-Scharr, A., Maenhaut, W., McFiggans, G., Mentel, T. F., Monod, A., Prévôt, A. S. H., Seinfeld, J. H., Surratt, J. D., Szmigielski, R., and Wildt, J.: The formation, properties and impact of secondary organic aerosol: current and emerging issues, *Atmos. Chem. Phys.*, 9, 5155-5236, 10.5194/acp-9-5155-2009, 2009.
- 670 Hildebrandt Ruiz, L., Paciga, A., Cerully, K., Nenes, A., Donahue, N., and Pandis, S.: Formation and aging of secondary organic aerosol from toluene: changes in chemical composition, volatility, and hygroscopicity, *Atmospheric Chemistry and Physics*, 15, 8301-8313, 10.5194/acp-15-8301-2015, 2015.
- 675 Hinks, M. L., Brady, M. V., Lignell, H., Song, M., Grayson, J. W., Bertram, A. K., Lin, P., Laskin, A., Laskin, J., and Nizkorodov, S. A.: Effect of viscosity on photodegradation rates in complex secondary organic aerosol materials, *Physical Chemistry Chemical Physics*, 18, 8785-8793, 10.1039/C5CP05226B, 2016.
- Hosny, N. A., Fitzgerald, C., Tong, C., Kalberer, M., Kuimova, M. K., and Pope, F. D.: Fluorescent lifetime imaging of atmospheric aerosols: a direct probe of aerosol viscosity, *Faraday Discussions*, 165, 343-356, 10.1039/c3fd00041a, 2013.
- 680 Houle, F. A., Hinsberg, W. D., and Wilson, K. R.: Oxidation of a model alkane aerosol by OH radical: the emergent nature of reactive uptake, *Physical Chemistry Chemical Physics*, 17, 4412-4423, 10.1039/c4cp05093b, 2015.
- Huff Hartz, K. E., Rosenørn, T., Ferchak, S. R., Raymond, T. M., Bilde, M., Donahue, N. M., and Pandis, S. N.: Cloud condensation nuclei activation of monoterpene and sesquiterpene secondary organic aerosol, *Journal of Geophysical Research: Atmospheres*, 110, n/a-n/a, 10.1029/2004jd005754, 2005.
- 685 Jacobson, K., Wu, E., and Poste, G.: Measurement of the translation mobility of concanavalin a in glycerol-saline solutions and on the cell surface by fluorescence recovery after photobleaching, *Biochimica et Biophysica Acta (BBA) - Biomembranes*, 433, 215-222, 10.1016/0005-2736(76)90189-9, 1976.
- Jain, S., Fischer, K. B., and Petrucci, G. A.: The Influence of Absolute Mass Loading of Secondary Organic Aerosols on Their Phase State, *Atmosphere*, 9, 10.3390/atmos9040131, 2018.
- 690 Jang, M., Ghio, A. J., and Cao, G.: Exposure of BEAS-2B Cells to Secondary Organic Aerosol Coated on Magnetic Nanoparticles, *Chemical research in toxicology*, 19, 1044-1050, 10.1021/tx0503597, 2006.
- Jimenez, J. L., Canagaratna, M. R., Donahue, N. M., Prevot, A. S. H., Zhang, Q., Kroll, J. H., DeCarlo, P. F., Allan, J. D., Coe, H., Ng, N. L., Aiken, A. C., Docherty, K. S., Ulbrich, I. M., Grieshop, A. P., Robinson, A. L., Duplissy, J., Smith, J. D., Wilson, K. R., Lanz, V. A., Hueglin, C., Sun, Y. L., Tian, J., Laaksonen, A., Raatikainen, T., Rautiainen, J., Vaattovaara, P., Ehn, M., Kulmala, M., Tomlinson, J. M., Collins, D. R., Cubison, M. J., Dunlea, J., Huffman, J. A., Onasch, T. B., Alfarra, M. R., Williams, P. I., Bower, K., Kondo, Y., Schneider, J., Drewnick, F., Borrmann, S., Weimer, S., Demerjian, K., Salcedo, D., Cottrell, L., Griffin, R., Takami, A., Miyoshi, T., Hatakeyama, S., Shimono, A., Sun, J. Y., Zhang, Y. M., Dzepina, K., Kimmel, J. R., Sueper, D., Jayne, J. T., Herndon, S. C., Trimborn, A. M., Williams, L. R., Wood, E. C., Middlebrook, A. M., Kolb, C. E., Baltensperger, U., and Worsnop, D. R.: Evolution of Organic Aerosols in the Atmosphere, *Science*, 326, 1525-1529, 10.1126/science.1180353, 2009.
- 700 Kanakidou, M., Seinfeld, J. H., Pandis, S. N., Barnes, I., Dentener, F. J., Facchini, M. C., Van Dingenen, R., Ervens, B., Nenes, A., Nielsen, C. J., Swietlicki, E., Putaud, J. P., Balkanski, Y., Fuzzi, S., Horth, J., Moortgat, G. K., Winterhalter, R., Myhre,

- C. E. L., Tsigaridis, K., Vignati, E., Stephanou, E. G., and Wilson, J.: Organic aerosol and global climate modelling: a review, *Atmos. Chem. Phys.*, 5, 1053-1123, 10.5194/acp-5-1053-2005, 2005.
- 705 Knopf, D. A.: Thermodynamic properties and nucleation processes of upper tropospheric and lower stratospheric aerosol particles, Diss. ETH No. 15103, Zurich, Switzerland, 2003.
- Koop, T., Kapilashrami, A., Molina, L. T., and Molina, M. J.: Phase transitions of sea-salt/water mixtures at low temperatures: Implications for ozone chemistry in the polar marine boundary layer, *Journal of Geophysical Research: Atmospheres*, 105, 26393-26402, 10.1029/2000jd900413, 2000.
- 710 Koop, T., Bookhold, J., Shiraiwa, M., and Pöschl, U.: Glass transition and phase state of organic compounds: dependency on molecular properties and implications for secondary organic aerosols in the atmosphere, *Physical Chemistry Chemical Physics*, 13, 19238-19255, 10.1039/c1cp22617g, 2011.
- Laskin, A., Laskin, J., and Nizkorodov, S. A.: Chemistry of Atmospheric Brown Carbon, *Chemical Reviews*, 115, 4335-4382, 10.1021/cr5006167, 2015.
- 715 Laskin, J., Laskin, A., Roach, P. J., Slysz, G. W., Anderson, G. A., Nizkorodov, S. A., Bones, D. L., and Nguyen, L. Q.: High-Resolution Desorption Electrospray Ionization Mass Spectrometry for Chemical Characterization of Organic Aerosols, *Analytical Chemistry*, 82, 2048-2058, 10.1021/ac902801f, 2010.
- Lee, H. D., Ray, K. K., and Tivanski, A. V.: Solid, Semisolid, and Liquid Phase States of Individual Submicrometer Particles Directly Probed Using Atomic Force Microscopy, *Analytical Chemistry*, 89, 12720-12726, 10.1021/acs.analchem.7b02755, 2017.
- 720 Lee, H. J., Laskin, A., Laskin, J., and Nizkorodov, S. A.: Excitation-Emission Spectra and Fluorescence Quantum Yields for Fresh and Aged Biogenic Secondary Organic Aerosols, *Environmental Science & Technology*, 47, 5763-5770, 10.1021/es400644c, 2013.
- Li, Y. J., Liu, P., Gong, Z., Wang, Y., Bateman, A. P., Bergoend, C., Bertram, A. K., and Martin, S. T.: Chemical Reactivity and Liquid/Nonliquid States of Secondary Organic Material, *Environmental Science & Technology*, 49, 13264-13274, 10.1021/acs.est.5b03392, 2015.
- 725 Lignell, H., Hinks, M. L., and Nizkorodov, S. A.: Exploring matrix effects on photochemistry of organic aerosols, *Proceedings of the National Academy of Sciences*, 111, 13780-13785, 10.1073/pnas.1322106111, 2014.
- Liu, P., Li, Y. J., Wang, Y., Gilles, M. K., Zaveri, R. A., Bertram, A. K., and Martin, S. T.: Lability of secondary organic particulate matter, *Proceedings of the National Academy of Sciences*, 113, 12643-12648, 10.1073/pnas.1603138113, 2016.
- 730 Longinotti, M. P., and Corti, H. R.: Diffusion of ferrocene methanol in super-cooled aqueous solutions using cylindrical microelectrodes, *Electrochemistry Communications*, 9, 1444-1450, <http://dx.doi.org/10.1016/j.elecom.2007.02.003>, 2007.
- Macleán, A. M., Butenhoff, C. L., Grayson, J. W., Barsanti, K., Jimenez, J. L., and Bertram, A. K.: Mixing times of organic molecules within secondary organic aerosol particles: a global planetary boundary layer perspective, *Atmos. Chem. Phys.*, 17, 13037-13048, 10.5194/acp-17-13037-2017, 2017.
- 735 Marsh, A., Rovelli, G., Song, Y.-C., Pereira, K. L., Willoughby, R. E., Bzdek, B. R., Hamilton, J. F., Orr-Ewing, A. J., Topping, D. O., and Reid, J. P.: Accurate representations of the physicochemical properties of atmospheric aerosols: when are laboratory measurements of value?, *Faraday Discussions*, 200, 639-661, 2017.
- Massoli, P., Lambe, A. T., Ahern, A. T., Williams, L. R., Ehn, M., Mikkilä, J., Canagaratna, M. R., Brune, W. H., Onasch, T. B., Jayne, J. T., Petäjä, T., Kulmala, M., Laaksonen, A., Kolb, C. E., Davidovits, P., and Worsnop, D. R.: Relationship between aerosol oxidation level and hygroscopic properties of laboratory generated secondary organic aerosol (SOA) particles, *Geophysical Research Letters*, 37, n/a-n/a, 10.1029/2010gl045258, 2010.
- 740 Meyvis, T. L., De Smedt, S., Van Oostveldt, P., and Demeester, J.: Fluorescence Recovery After Photobleaching: A Versatile Tool for Mobility and Interaction Measurements in Pharmaceutical Research, *Pharm Res*, 16, 1153-1162, 10.1023/a:1011924909138, 1999.
- 745 Mikhailov, E., Vlasenko, S., Martin, S., Koop, T., and Pöschl, U.: Amorphous and crystalline aerosol particles interacting with water vapor: conceptual framework and experimental evidence for restructuring, phase transitions and kinetic limitations, *Atmospheric Chemistry and Physics*, 9, 9491-9522, 2009.
- Murray, B. J., Wilson, T. W., Dobbie, S., Cui, Z., Al-Jumur, S. M. R. K., Mohler, O., Schnaiter, M., Wagner, R., Benz, S., 750 Niemand, M., Saathoff, H., Ebert, V., Wagner, S., and Karcher, B.: Heterogeneous nucleation of ice particles on glassy aerosols under cirrus conditions, *Nature Geosci*, 3, 233-237, 10.1038/ngeo817, 2010.

- Nguyen, T. B., Laskin, A., Laskin, J., and Nizkorodov, S. A.: Brown carbon formation from ketoaldehydes of biogenic monoterpenes, *Faraday Discussions*, 165, 473-494, 10.1039/c3fd00036b, 2013.
- 755 Nozière, B., Kalberer, M., Claeys, M., Allan, J., D'Anna, B., Decesari, S., Finessi, E., Glasius, M., Grgić, I., Hamilton, J. F., Hoffmann, T., Iinuma, Y., Jaoui, M., Kahnt, A., Kampf, C. J., Kourchev, I., Maenhaut, W., Marsden, N., Saarikoski, S., Schnelle-Kreis, J., Surratt, J. D., Szidat, S., Szmigielski, R., and Wisthaler, A.: The Molecular Identification of Organic Compounds in the Atmosphere: State of the Art and Challenges, *Chemical Reviews*, 115, 3919-3983, 10.1021/cr5003485, 2015.
- 760 Perraud, V., Bruns, E. A., Ezell, M. J., Johnson, S. N., Yu, Y., Alexander, M. L., Zelenyuk, A., Imre, D., Chang, W. L., Dabdub, D., Pankow, J. F., and Finlayson-Pitts, B. J.: Nonequilibrium atmospheric secondary organic aerosol formation and growth, *Proceedings of the National Academy of Sciences*, 109, 2836-2841, 10.1073/pnas.1119909109, 2012.
- Poschl, U., and Shiraiwa, M.: Multiphase Chemistry at the Atmosphere-Biosphere Interface Influencing Climate and Public Health in the Anthropocene, *Chemical Reviews*, 115, 4440-4475, 10.1021/cr500487s, 2015.
- 765 Power, R. M., Simpson, S. H., Reid, J. P., and Hudson, A. J.: The transition from liquid to solid-like behaviour in ultrahigh viscosity aerosol particles, *Chemical Science*, 4, 2597-2604, 10.1039/c3sc50682g, 2013.
- Price, H. C., Mattsson, J., Zhang, Y., Bertram, A. K., Davies, J. F., Grayson, J. W., Martin, S. T., O'Sullivan, D., Reid, J. P., and Rickards, A. M.: Water diffusion in atmospherically relevant α -pinene secondary organic material, *Chemical Science*, 6, 4876-4883, 2015.
- 770 Price, H. C., Mattsson, J., and Murray, B. J.: Sucrose diffusion in aqueous solution, *Physical Chemistry Chemical Physics*, 18, 19207-19216, 10.1039/C6CP03238A, 2016.
- Pye, H. O. T., Chan, A. W. H., Barkley, M. P., and Seinfeld, J. H.: Global modeling of organic aerosol: the importance of reactive nitrogen (NO_x and NO₃), *Atmos. Chem. Phys.*, 10, 11261-11276, 10.5194/acp-10-11261-2010, 2010.
- Reid, J. P., Bertram, A. K., Topping, D. O., Laskin, A., Martin, S. T., Petters, M. D., Pope, F. D., and Rovelli, G.: The viscosity of atmospherically relevant organic particles, *Nature Communications*, 9, 956, 10.1038/s41467-018-03027-z, 2018.
- 775 Renbaum-Wolff, L., Grayson, J. W., Bateman, A. P., Kuwata, M., Sellier, M., Murray, B. J., Shilling, J. E., Martin, S. T., and Bertram, A. K.: Viscosity of α -pinene secondary organic material and implications for particle growth and reactivity, *Proceedings of the National Academy of Sciences*, 110, 8014-8019, 10.1073/pnas.1219548110, 2013a.
- Renbaum-Wolff, L., Grayson, J. W., and Bertram, A. K.: Technical Note: New methodology for measuring viscosities in small volumes characteristic of environmental chamber particle samples, *Atmos. Chem. Phys.*, 13, 791-802, 10.5194/acp-13-791-2013, 2013b.
- 780 Riipinen, I., Pierce, J., Yli-Juuti, T., Nieminen, T., Hakkinen, S., Ehn, M., Junninen, H., Lehtipalo, K., Petaja, T., and Slowik, J.: Organic condensation: a vital link connecting aerosol formation to cloud condensation nuclei (CCN) concentrations, *Atmospheric Chemistry and Physics*, 11, 3865, 10.5194/acp-11-3865-2011, 2011.
- 785 Robinson, C. B., Schill, G. P., and Tolbert, M. A.: Optical growth of highly viscous organic/sulfate particles, *Journal of Atmospheric Chemistry*, 71, 145-156, 10.1007/s10874-014-9287-8, 2014.
- Saathoff, H., Naumann, K. H., Möhler, O., Jonsson, Å. M., Hallquist, M., Kiendler-Scharr, A., Mentel, T. F., Tillmann, R., and Schurath, U.: Temperature dependence of yields of secondary organic aerosols from the ozonolysis of α -pinene and limonene, *Atmos. Chem. Phys.*, 9, 1551-1577, 10.5194/acp-9-1551-2009, 2009.
- 790 Schneider, C. A., Rasband, W. S., and Eliceiri, K. W.: NIH Image to ImageJ: 25 years of image analysis, *Nat methods*, 9, 671-675, 2012.
- Seinfeld, J. H., and Pandis, S. N.: *Atmospheric chemistry and physics: from air pollution to climate change*, John Wiley & Sons, 2016.
- Seksek, O., Biwersi, J., and Verkman, A. S.: Translational Diffusion of Macromolecule-sized Solutes in Cytoplasm and Nucleus, *The Journal of Cell Biology*, 138, 131-142, 10.1083/jcb.138.1.131, 1997.
- 795 Shiraiwa, M., Ammann, M., Koop, T., and Pöschl, U.: Gas uptake and chemical aging of semisolid organic aerosol particles, *Proceedings of the National Academy of Sciences*, 108, 11003-11008, 10.1073/pnas.1103045108, 2011.
- Shiraiwa, M., and Seinfeld, J. H.: Equilibration timescale of atmospheric secondary organic aerosol partitioning, *Geophysical Research Letters*, 39, n/a-n/a, 10.1029/2012gl054008, 2012.
- 800 Shiraiwa, M., Zuend, A., Bertram, A. K., and Seinfeld, J. H.: Gas-particle partitioning of atmospheric aerosols: interplay of physical state, non-ideal mixing and morphology, *Physical Chemistry Chemical Physics*, 15, 11441-11453, 2013.

- Shiraiwa, M., Li, Y., Tsimpidi, A. P., Karydis, V. A., Berkemeier, T., Pandis, S. N., Lelieveld, J., Koop, T., and Pöschl, U.: Global distribution of particle phase state in atmospheric secondary organic aerosols, *Nature Communications*, 8, 15002, 10.1038/ncomms15002
<https://www.nature.com/articles/ncomms15002#supplementary-information>, 2017a.
- 805 Shiraiwa, M., Ueda, K., Pozzer, A., Lammel, G., Kampf, C. J., Fushimi, A., Enami, S., Arangio, A. M., Frohlich-Nowoisky, J., Fujitani, Y., Furuyama, A., Lakey, P. S. J., Lelieveld, J., Lucas, K., Morino, Y., Poschl, U., Takaharna, S., Takami, A., Tong, H. J., Weber, B., Yoshino, A., and Sato, K.: Aerosol Health Effects from Molecular to Global Scales, *Environmental Science & Technology*, 51, 13545-13567, 10.1021/acs.est.7b04417, 2017b.
- 810 Shrivastava, M., Cappa, C. D., Fan, J., Goldstein, A. H., Guenther, A. B., Jimenez, J. L., Kuang, C., Laskin, A., Martin, S. T., Ng, N. L., Petaja, T., Pierce, J. R., Rasch, P. J., Roldin, P., Seinfeld, J. H., Shilling, J., Smith, J. N., Thornton, J. A., Volkamer, R., Wang, J., Worsnop, D. R., Zaveri, R. A., Zelenyuk, A., and Zhang, Q.: Recent advances in understanding secondary organic aerosol: Implications for global climate forcing, *Reviews of Geophysics*, 55, 509-559, 10.1002/2016rg000540, 2017a.
- 815 Shrivastava, M., Lou, S., Zelenyuk, A., Easter, R. C., Corley, R. A., Thrall, B. D., Rasch, P. J., Fast, J. D., Massey Simonich, S. L., Shen, H., and Tao, S.: Global long-range transport and lung cancer risk from polycyclic aromatic hydrocarbons shielded by coatings of organic aerosol, *Proceedings of the National Academy of Sciences*, 114, 1246-1251, 10.1073/pnas.1618475114, 2017b.
- Sindelarova, K., Granier, C., Bouarar, I., Guenther, A., Tilmes, S., Stavrou, T., Muller, J. F., Kuhn, U., Stefani, P., and Knorr, W.: Global data set of biogenic VOC emissions calculated by the MEGAN model over the last 30 years, *Atmospheric Chemistry and Physics*, 14, 9317-9341, 10.5194/acp-14-9317-2014, 2014.
- 820 Sinnecker, D., Voigt, P., Hellwig, N., and Schaefer, M.: Reversible Photobleaching of Enhanced Green Fluorescent Proteins, *Biochemistry*, 44, 7085-7094, 10.1021/bi047881x, 2005.
- Solomon, S.: *Climate change 2007-the physical science basis: Working group I contribution to the fourth assessment report of the IPCC*, Cambridge University Press, 2007.
- 825 Solomon, S., D. Qin, M. Manning, Z. Chen, M. Marquis, K.B. Averyt, M. Tignor and, and (eds.), H. L. M.: *IPCC Fourth Assessment Report: Climate Change 2007: The Physical Science Basis: Contribution of Working Group I to the Fourth Assessment Report of the Intergovernmental Panel on Climate Change*, Cambridge University Press, Cambridge, United Kingdom and New York, NY, USA, 996 pp., 2007.
- Song, M., Liu, P. F., Hanna, S. J., Li, Y. J., Martin, S. T., and Bertram, A. K.: Relative humidity-dependent viscosities of isoprene-derived secondary organic material and atmospheric implications for isoprene-dominant forests, *Atmos. Chem. Phys.*, 15, 5145-5159, 10.5194/acp-15-5145-2015, 2015.
- 830 Song, M., Liu, P. F., Hanna, S. J., Zaveri, R. A., Potter, K., You, Y., Martin, S. T., and Bertram, A. K.: Relative humidity-dependent viscosity of secondary organic material from toluene photo-oxidation and possible implications for organic particulate matter over megacities, *Atmospheric Chemistry and Physics*, 16, 8817-8830, 10.5194/acp-16-8817-2016, 2016.
- 835 Spracklen, D. V., Jimenez, J. L., Carslaw, K. S., Worsnop, D. R., Evans, M. J., Mann, G. W., Zhang, Q., Canagaratna, M. R., Allan, J., Coe, H., McFiggans, G., Rap, A., and Forster, P.: Aerosol mass spectrometer constraint on the global secondary organic aerosol budget, *Atmos. Chem. Phys.*, 11, 12109-12136, 10.5194/acp-11-12109-2011, 2011.
- Stout, A. L., and Axelrod, D.: SPONTANEOUS RECOVERY OF FLUORESCENCE BY PHOTOBLEACHED SURFACE-ADSORBED PROTEINS, *Photochemistry and Photobiology*, 62, 239-244, 10.1111/j.1751-1097.1995.tb05264.x, 1995.
- 840 Taina, Y. J., Aki, P., Olli-Pekka, T., Angela, B., Celia, F., Olli, V., Liqing, H., Eetu, K., Otso, P., Olga, G., Manabu, S., Mikael, E., Kari, L., and Annele, V.: Factors controlling the evaporation of secondary organic aerosol from α -pinene ozonolysis, *Geophysical Research Letters*, 44, 2562-2570, doi:10.1002/2016GL072364, 2017.
- Verkman, A. S.: [28] Diffusion in cells measured by fluorescence recovery after photobleaching, *Methods in Enzymology*, 360, 635-648, 10.1016/S0076-6879(03)60132-1, 2003.
- 845 Wagner, R., Höhler, K., Huang, W., Kiselev, A., Möhler, O., Mohr, C., Pajunoja, A., Saathoff, H., Schiebel, T., and Shen, X.: Heterogeneous ice nucleation of α -pinene SOA particles before and after ice cloud processing, *Journal of Geophysical Research: Atmospheres*, 122, 4924-4943, 2017.
- Wang, B., Lambe, A. T., Massoli, P., Onasch, T. B., Davidovits, P., Worsnop, D. R., and Knopf, D. A.: The deposition ice nucleation and immersion freezing potential of amorphous secondary organic aerosol: Pathways for ice and mixed-phase cloud formation, *Journal of Geophysical Research: Atmospheres*, 117, n/a-n/a, 10.1029/2012jd018063, 2012.

- 850 Wang, B., O'Brien, R. E., Kelly, S. T., Shilling, J. E., Moffet, R. C., Gilles, M. K., and Laskin, A.: Reactivity of Liquid and Semisolid Secondary Organic Carbon with Chloride and Nitrate in Atmospheric Aerosols, *The Journal of Physical Chemistry A*, 119, 4498-4508, 10.1021/jp510336q, 2015.
- Ye, Q., Robinson, E. S., Ding, X., Ye, P., Sullivan, R. C., and Donahue, N. M.: Mixing of secondary organic aerosols versus relative humidity, *Proceedings of the National Academy of Sciences*, 113, 12649-12654, 10.1073/pnas.1604536113, 2016.
- 855 Ye, Q., Upshur, M. A., Robinson, E. S., Geiger, F. M., Sullivan, R. C., Thomson, R. J., and Donahue, N. M.: Following Particle-Particle Mixing in Atmospheric Secondary Organic Aerosols by Using Isotopically Labeled Terpenes, *Chem*, 4, 318-333, 10.1016/j.chempr.2017.12.008, 2018.
- Zaveri, R. A., Easter, R. C., Shilling, J. E., and Seinfeld, J. H.: Modeling kinetic partitioning of secondary organic aerosol and size distribution dynamics: representing effects of volatility, phase state, and particle-phase reaction, *Atmos. Chem. Phys.*, 14, 5153-5181, 10.5194/acp-14-5153-2014, 2014.
- 860 Zaveri, R. A., Shilling, J. E., Zelenyuk, A., Liu, J., Bell, D. M., D'Ambro, E. L., Gaston, C. J., Thornton, J. A., Laskin, A., Lin, P., Wilson, J., Easter, R. C., Wang, J., Bertram, A. K., Martin, S. T., Seinfeld, J. H., and Worsnop, D. R.: Growth Kinetics and Size Distribution Dynamics of Viscous Secondary Organic Aerosol, *Environmental Science & Technology*, 52, 1191-1199, 10.1021/acs.est.7b04623, 2018.
- 865 Zelenyuk, A., Imre, D., Beránek, J., Abramson, E., Wilson, J., and Shrivastava, M.: Synergy between Secondary Organic Aerosols and Long-Range Transport of Polycyclic Aromatic Hydrocarbons, *Environmental Science & Technology*, 46, 12459-12466, 10.1021/es302743z, 2012.
- Zhang, Y., Sanchez, M. S., Douet, C., Wang, Y., Bateman, A. P., Gong, Z., Kuwata, M., Renbaum-Wolff, L., Sato, B. B., Liu, P. F., Bertram, A. K., Geiger, F. M., and Martin, S. T.: Changing shapes and implied viscosities of suspended submicron particles, *Atmos. Chem. Phys.*, 15, 7819-7829, 10.5194/acp-15-7819-2015, 2015.
- 870 Zhou, S., Lee, A. K. Y., McWhinney, R. D., and Abbatt, J. P. D.: Burial Effects of Organic Coatings on the Heterogeneous Reactivity of Particle-Borne Benzo[a]pyrene (BaP) toward Ozone, *The Journal of Physical Chemistry A*, 116, 7050-7056, 10.1021/jp3030705, 2012.
- Zobrist, B., Soonsin, V., Luo, B. P., Krieger, U. K., Marcolli, C., Peter, T., and Koop, T.: Ultra-slow water diffusion in aqueous sucrose glasses, *Physical Chemistry Chemical Physics*, 13, 3514-3526, 10.1039/C0CP01273D, 2011.
- 875